



Synthesis of silver and copper oxide nanoparticles using *Myristica fragrans* fruit extract: Antimicrobial and catalytic applications

Drishya Sasidharan^a, T.R. Namitha^a, Smera P. Johnson^a, Vimala Jose^b, Paulson Mathew^{a,*}

^a Department of Chemistry, Centre for Sustainability Science, St. Thomas College, Calicut University, Thrissur, 680001, Kerala, India

^b Department of Botany, St. Thomas College (Autonomous), Calicut University, Thrissur, 680001, Kerala, India

ARTICLE INFO

Keywords:

Myristica fragrans
Copper oxide nanoparticle
Silver nanoparticle
Click reaction
Antibacterial activity

ABSTRACT

The pericarp of *Myristica fragrans* fruit extract was utilized for a low cost, eco-friendly synthesis of silver (AgNPs) and copper oxide (CuONPs) nanoparticles. The aqueous fruit extract of the plant was used as reducing and stabilizing agents for this preparation. Characterization of the biosynthesized nanoparticles was carried out using UV–Vis spectroscopy, FTIR spectroscopy and X-Ray Diffraction studies. Morphology and size of the particles was observed using Field-Emission Scanning Electron Microscopy (FESEM) and High Resolution Transmission Electron Microscopy (HRTEM). The copper and silver nanoparticles show Surface Plasmon Resonance (SPR) band at 360 and 478 nm respectively in the UV–Vis spectrum. It was observed that size of the synthesized copper oxide and silver nanoparticles are in the range 10–50 nm. The presence of copper and silver elements was confirmed from their respective EDS spectrum. Involvement of phytochemicals in the stabilization and reduction of the nanoparticles was confirmed by FTIR spectroscopy. CuONPs exhibited catalytic activity in 1,3-dipolar cycloaddition reaction between azides and terminal alkynes to form 1,2,3-triazoles. Silver nanoparticle possesses good antibacterial activity against multidrug human pathogens *Escherichia coli*, *Pseudomonas aeruginosa*, *Staphylococcus aureus* and *Bacillus subtilis*. The present study focuses on the utilization of the less economic part of *Myristica fragrans* fruit's pericarp for the preparation of copper oxide and silver nanoparticles which have good catalytic and antibacterial activities.

1. Introduction

For the last two decades, nanomaterials have gained much attention due to their interesting properties that can be attributed to the change in geometry, size, shape, and morphology when compared with bulk materials (Thangavel and Ramaraj, 2008; Nadagouda and Varma, 2006). Moreover, nanotechnology and natural science offer diverse and easy biosynthetic pathways that can extend the application of nanoparticles in catalysis, pollution control, agriculture, waste management, and in the biomedical field as antimicrobial, anticancer agents (Lewinski et al., 2008). Among the metal nanoparticles, copper and silver nanoparticles are comparatively more important due to their wide range of applications in biology (Nasrollahzadeh et al., 2019a,b). They are known to have a broad range of antimicrobial properties and most of them are not detrimental to human health (Koduru et al., 2018). Biosynthesis of nanoparticles is generally a bottom-up approach involving reduction and oxidation reactions which utilise plant extracts, bacteria, fungi as raw materials (Hebbalalu et al., 2013). Although the exact synthetic

mechanism is still unknown, synthesis of nanoparticles requires the presence of reducing and stabilizing agents where the organic molecules are able to handle both the roles. Metal oxide nanoparticle possesses exclusive chemical and physical properties because of their high density and surface area. Developing environmentally benign methods for the synthesis of metal nanoparticles relies on the utilization of non toxic chemicals (Anastas and Kirchhoff, 2002). Use of microwave has emerged as an effective tool in synthesis of nanoparticles in aqueous media (Baruwati et al., 2009; Kou and Varma, 2012). Such green chemistry protocols protect the environment by reducing waste by utilizing renewable sources and energy efficiency (Baruwati and Varma, 2009).

Plant extract mediated synthesis of nanoparticles has been copiously reported in the recently. (Saratale et al., 2018). Nanoparticles have been synthesized from bio-resources utilizing the rich reservoir of alkaloids and flavonoids present in it (Nadagouda and Varma, 2008; Nadagouda et al., 2014). Such green nanoparticle synthesis is simple and possesses innumerable applications (Varma, 2012; Abdelghany et al., 2018).

* Corresponding author.

E-mail address: paulsonmathew@stthomas.ac.in (P. Mathew).

<https://doi.org/10.1016/j.scp.2020.100255>

Received 13 October 2019; Received in revised form 21 February 2020; Accepted 29 March 2020

Available online 18 April 2020

2352-5541/© 2020 Elsevier B.V. All rights reserved.

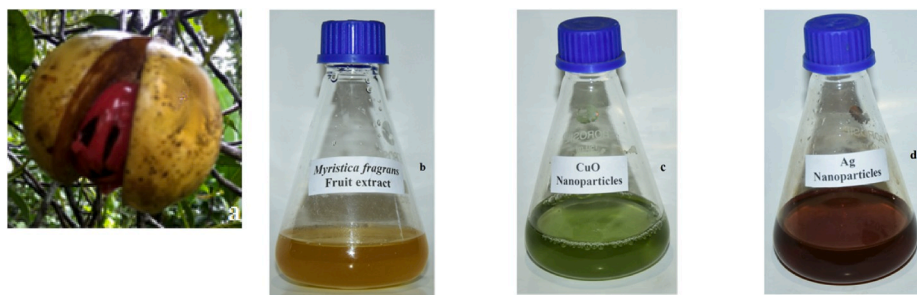


Fig. 1. (a) *Myristica fragrans* fruit (b) extract of the pericarp (c) copper oxide nanoparticles in solution and (d) silver nanoparticles in solution.

Biological applications of such nanoparticles include their potential cytotoxicity towards different cancerous cells (Jadhav et al., 2018a,b), antimicrobial power (Zheng et al., 2018), antioxidant, DNA cleavage properties (Jadhav et al., 2018a,b) and anticoagulant capacity (Tian et al., 2014). Metal oxide nanoparticle found out its application in optoelectronics (Yu et al., 2016), sensors (Cho et al., 2017) and in fuel cells (Sun et al., 2019). They have been also used in biomedical and environmental sensors (Belushkin et al., 2018). In addition to the above applications, silver nanoparticles are widely used in degradation of dyes (Polepalli and Rao, 2018) and in mosquito control (Sooresh et al., 2011). However, there are only a few reports on the catalytic activity of nanoparticles synthesized using plant materials (Xia et al., 2013; Nasrollahzadeh et al., 2019a,b).

Conventionally, Huisgen's 1,3-dipolar cycloaddition reaction between azide and alkyne was utilized for the construction of triazole ring. This uncatalyzed reaction required high temperature but was slow in nature affording both 1,4- and 1,5-disubstituted triazoles in equal amounts (Huisgen, 1963). Introduction of copper (I) species as a catalyst for the regioselective synthesis of the 1,4-isomer has received wide attention after the work of Sharpless (Kolb et al., 2001), who coined the term Click Chemistry. It has a wide range of applications in organic chemistry (Bock et al., 2006; Meldal et al., 2017), medicinal chemistry (Anseth and Klok, 2016), polymers, material sciences (Lutz, 2007) and bioconjugation (Lutz and Zarafshani, 2008). Development of new synthetic protocols using principles of green chemistry are much sought after. In this context, green synthesis of metal nanoparticles using bio-sources has been suggested.

Myristica fragrans belongs to the family Myristicaceae, the source of the spices nutmeg and mace. Outer pericarp of the fruit possesses little commercial value and is usually thrown away after extracting the seed and aril. *Myristica fragrans* fruit is used for the treatment of digestive disorders in traditional medicines (Acuña et al., 2016). Its extract possesses antioxidant and anti-inflammatory properties and has been widely used in food industry (e.g., jam, pickle, cake, and jelly) and in beverage preparations (Sulaiman and Ooi, 2012). The pharmacological evaluation reveals that aqueous extract of the pericarp contains terpenoids, flavones, phenols, tannins, sugars etc. (Zhao et al., 2019; Pandey et al., 2016). In the present study, extract of the pericarp was used for preparing copper oxide and silver nanoparticles. The synthesized nanoparticles were well characterized. Further, the efficiency of copper oxide nanoparticle towards catalyzing the click reaction for the regioselective synthesis of 1,4-disubstituted 1,2,3-triazoles and antimicrobial activity of the silver nanoparticle by disc diffusion method was investigated.

2. Materials and methods

2.1. Plant material collection and processing

Myristica fragrans fruit (Fig. 1a) was collected from Thrissur, Kerala. The fruit was washed with distilled water and its pericarp (500 g) was separated from the seed. The pericarp was dried well under sun shade

for four days to remove the moisture content and crushed into small pieces. It was boiled with water and the extract thus obtained was used for the synthesis of CuO and silver nanoparticles.

2.2. Characterization

All the reagents used were purchased from Merck chemicals, Bangalore, India, unless otherwise mentioned. The absorption spectra of the nanoparticles were recorded using Shimadzu UV-1800 series spectrometer. Field Emission Gun-Scanning electron microscope (JEOL Model JSM-7600F) was used to study the surface morphology of the nanoparticles. Interaction of specific functional groups present in the phytochemicals was studied using Shimadzu IR Affinity 1 Spectrometer. Size of the nanoparticle was determined using Jeol/JEM 2100 HRTEM and powder X-ray diffraction was performed using PANalytical diffractometer. GCMS studies were conducted in an ISQ LT GC-MS Thermo Fisher Scientific instrument.

2.3. Preparation of the fruit extract

For preparing the fruit extract, 10 g of the grounded dried nutmeg fruit's pericarp was transferred into a reaction vessel. Deionized water (50 ml) was added to it and boiled for 1 h at 100 °C. After cooling the solution to room temperature, it was filtered using Whatman no.1 filter paper. The residue was washed with water (20 mL) and the combined filtrates were made up to 100 mL and stored at 4 °C.

2.4. Synthesis of CuO nanoparticles

To a stirred solution of copper acetate (10 mM, 90 mL), *Myristica fragrans* fruit extract (10 mL) was added at room temperature. Stirring was continued for 10 min followed by microwave irradiation (Koryo multi-mate) at a power of 800 W and frequency of 2450 MHz for 5 min, maintaining a temperature below 100 °C. Under microwave heating, the solution changes its color from blue to green and finally to a greenish brown suspension. The CuO nanoparticles formed were recovered by centrifugation and washed with deionized water. The residue obtained was dried in a vacuum oven at 70 °C for 6 h.

2.5. Synthesis of silver nanoparticles

An aqueous solution of silver nitrate (10 mmol, 90 mL) was mixed with *Myristica fragrans* fruit extract (10 mL). On exposure to sunlight, the solution changes its colour from yellow to reddish brown within 10 min. The nanoparticles thus formed were recovered by centrifugation and washed with deionized water. The residue obtained was dried in a vacuum oven at 70 °C for 6 h.

2.6. Synthesis of 1,2,3-triazole using CuO nanoparticle

To a mixture of azide (1.5 mmol), alkyne (1.5 mmol) and halide (1 mmol) in distilled water (5 mL), CuONPs (10 mg) was added. The

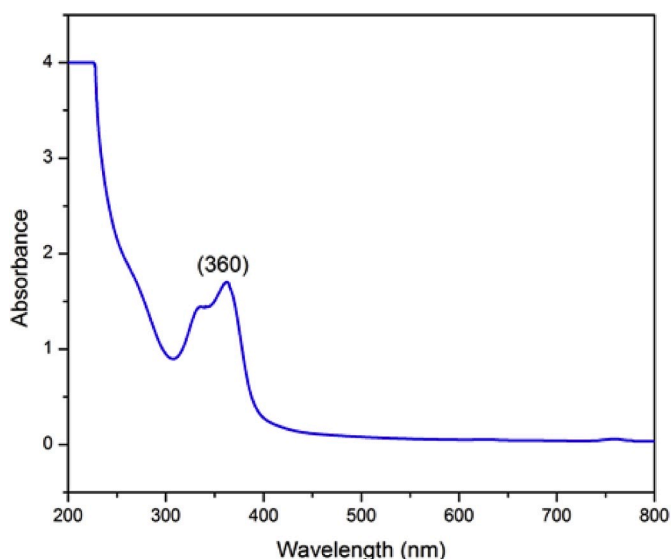


Fig. 2a. UV-Visible spectrum of CuO nanoparticles.

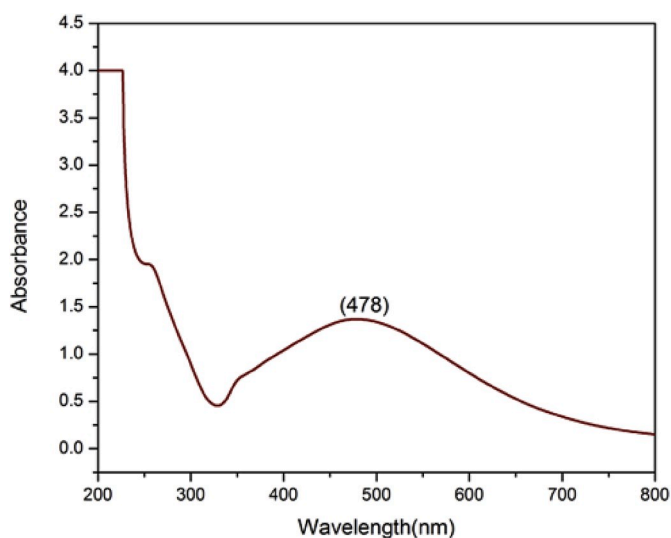


Fig. 2b. UV-Visible spectrum of Ag NPs.

reaction mixture was heated at 60 °C for 1 h with stirring. After cooling to room temperature, the solid formed was separated by filtration and recrystallised from ethanol to afford 1,2,3-triazoles in excellent yields.

2.7. Antibacterial activity of silver nanoparticles by disc diffusion method

Antibacterial activities of AgNPs were investigated by the agar disk diffusion method. Nutrient agar media 25 mL (Hi Media, Mumbai) was poured into sterilized petriplates under sterile conditions and left it to gel at room temperature. The culture suspensions from the pure cultures of gram-positive bacteria *Bacillus subtilis* (MTCC 869), *Staphylococcus aureus* (MTCC 3103) and gram-negative bacteria *Escherichia coli* (MTCC 68), *Pseudomonas aeruginosa* (2642) were chosen based on their clinical and pharmacological importance. The bacterial strains used for evaluating antimicrobial activity were obtained from the Institute of Microbial Technology, Chandigarh, India and maintained in nutrient broth. The sterile filter paper discs (6 mm diameter) were saturated with four different concentrations of AgNPs and streptomycin as the positive control. The filter paper discs were placed equidistantly on the inoculated media and diffusion of solution was allowed to occur for 30 min at room temperature. These plates were then incubated at 37 °C for 24 h

and the average zone of inhibition was recorded.

3. Results and discussion

3.1. Synthesis and characterization of CuO and Ag NPs

3.1.1. Synthesis of CuO and Ag NPs nanoparticles

For the phytosynthesis of copper and silver nanoparticles, aqueous fruit extract of *Myristica fragrans* was used (Fig. 1b). The fruit extract was added to copper acetate solution and the resulting solution was irradiated under microwave for 5 min. Colour of the solution changed from blue to bluish green and then to greenish brown suspension within this period of time which was a clear indication of the formation of copper oxide nanoparticles (Fig. 1c). Copper oxide nanoparticles thus obtained were separated by centrifugation at 7000 rpm for 30 min. Successive washing with water removed water-soluble impurities and the nanoparticles were dried in a vacuum oven at 70 °C. Direct synthesis of copper oxide nanoparticles by conventional heating for 2 h did not produce any nanoparticles.

When *Myristica fragrans* fruit extract was mixed with silver nitrate solution at room temperature or ambient temperature in dark conditions, it did not produce any characteristic color of silver nanoparticles even after 24 h. However, the solution changes its color from yellow to brown upon exposure to sunlight for 10 min, which is a clear indication of silver nanoparticle formation (Fig. 1d). In a separate experiment when the time of exposure to sunlight was extended for 30 min; a dark brown solution was obtained. The solution was centrifuged at 700 rpm for 30 min and water-soluble impurities were removed by successive washings. The nanoparticles were dried in a vacuum oven at 70 °C.

Formation of metal nanoparticles can be rationalized by the involvement of phytochemicals present in the aqueous extract of *Myristica fragrans* fruit extract as reducing and stabilizing agent. An ethyl acetate extract obtained from the aqueous extract of *Myristica fragrans* pericarp was subjected GC-MS analysis (Supporting Information Fig. S1). The chromatogram showed eugenol derivatives and fatty acids as the major constituents (Supporting Information Table S1).

3.1.2. UV-visible spectroscopy analysis

Addition of *Myristica fragrans* fruit extract induces a gradual color change of metal precursor solution from blue to bluish green and then to greenish brown suspension which was attributed to the formation of copper oxide nanoparticle. Surface Plasmon Resonance (SPR) was observed at λ 360 nm in the UV-visible spectrum (Fig. 2a). The UV-Visible spectrum of silver nanoparticle is shown in Fig. 2b. Brown color of the solution was attributed to the formation of silver nanoparticle and SPR of the solution was observed at λ 478 nm. The SPR originates from the oscillations of surface electrons of nanoparticles.

3.1.3. Infrared spectral analysis

Phytoconstituents present in the plant extract and the formation of metal oxide was identified using FTIR analysis. FTIR of the bio-synthesized CuO and silver nanoparticle is shown in Fig. 3. In Fig. 3a, the peaks observed at 497, 689 and 868 cm^{-1} corresponded to characteristic stretching frequencies of the copper oxides. The peaks at 713 cm^{-1} and 1384 cm^{-1} corresponded to alkanes and alkane C-H_{rocking} vibrations. Alkenic C-H bond vibration was observed at 975 cm^{-1} . Aromatic C=C stretching vibration was observed at 1556 cm^{-1} . Presence of the phenolic -OH group in the phytoconstituent was identified as the peak at 3238 cm^{-1} .

FTIR spectrum of the silver nanoparticle is shown in Fig. 3b. Out of plane bending vibration of aromatic C-H was observed at 673 cm^{-1} . Stretching vibration of ether functionality (C-O-C) and bending of CH₂ were observed at 1009 cm^{-1} and 1365 cm^{-1} respectively. Carbonyl (C=O) stretching vibration was observed at 1740 cm^{-1} . Stretching vibration of aliphatic C-H was observed at 2973 cm^{-1} and phenolic -OH at 3464 cm^{-1} . This confirms the association of eugenol derivatives and long

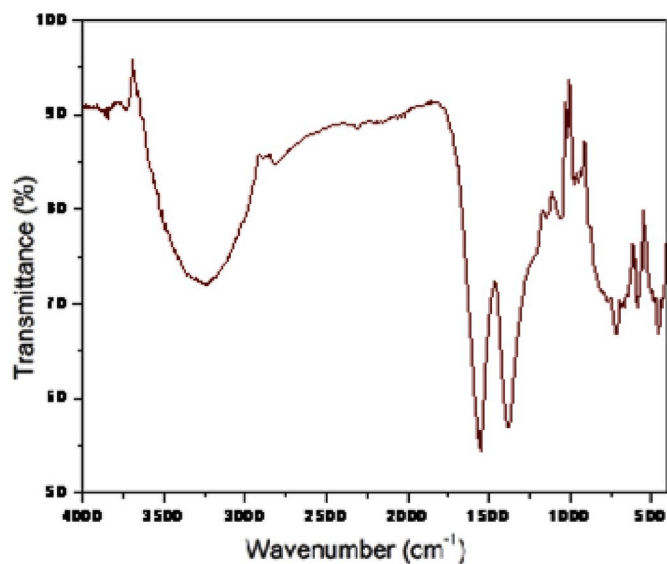


Fig. 3a. FTIR spectrum of CuO nanoparticles.

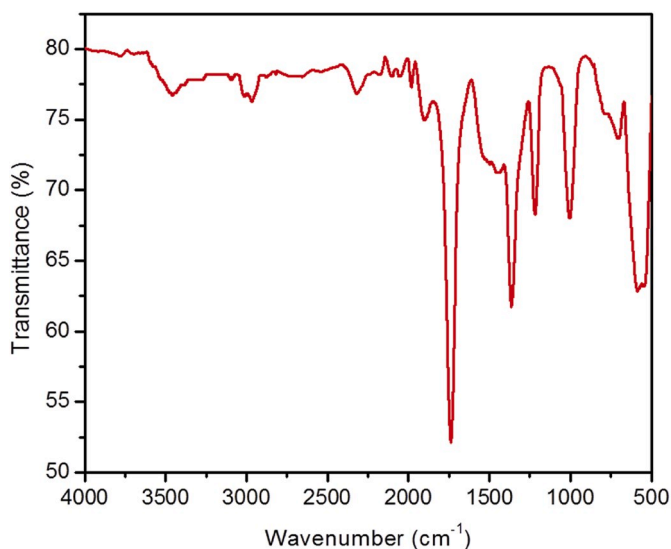


Fig. 3b. FTIR spectrum of silver nanoparticles.

chain fatty acids with the nanoparticles.

3.1.4. Powder X-ray diffraction analysis

The XRD pattern reveals the presence of CuO and silver nanoparticles (Fig. 4). In Fig. 4a, the 2θ values at 32.5° , 35.6° , 38.8° , 48.7° , 50.5° , 58.4° , 61.5° , 66.4° , 67.9° , 73.7° corresponds to (1 1 0), (1 1 -1), (1 1 1), (2 0 -2), (1 1 2), (2 0 2), (1 1 -3), (3 1 0), (1 1 3), (2 2 1) planes of CuO monoclinic phase (JCPDS No: 98-009-2367). Peaks at 29.7° , 42.4° correspond to (0 1 1), (0 0 2), planes of Cu₂O (JCPDS No: 96-900-5770) whereas the peak at 43.5° is attributed to (1 1 1) plane of Cu (JCPDS No: 04-0836). Presence of small amount of copper(I) oxide and copper(0) was observed as impurities possibly due to the over-reduction of CuO by the plant extract. Our attempts to exclude these Cu₂O impurities by this method were not successful. The nanoparticle is considered to be an agglomeration of two or more individual crystallites. From the Scherrer equation, the average crystallite size of copper oxide nanoparticles was calculated to be 15.7 nm.

The diffraction pattern of the silver nanoparticle is shown in Fig. 4b. Fig. 4b(A) is the diffractogram of the silver nanoparticles prepared after

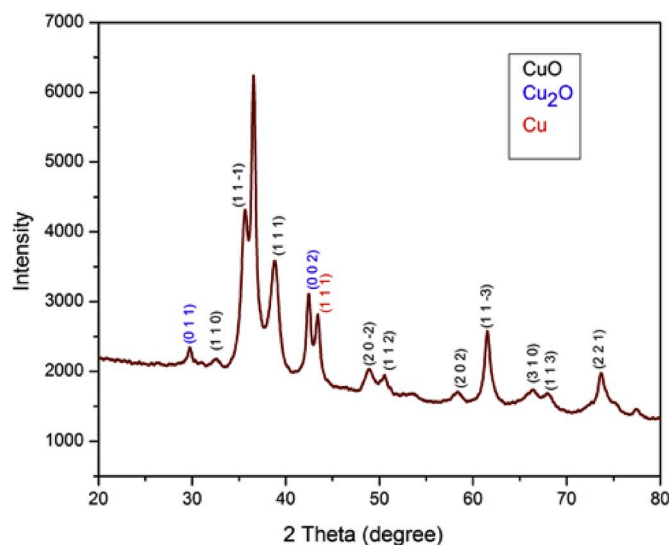


Fig. 4a. XRD pattern of CuO nanoparticles.

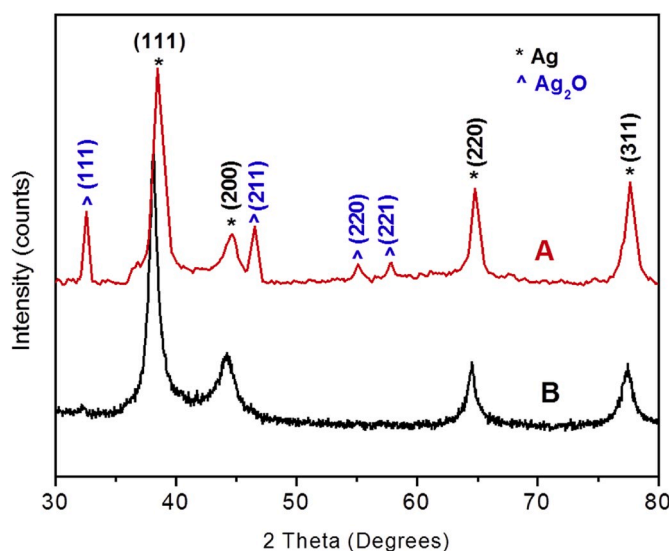


Fig. 4b. XRD pattern of AgNPs (A) after 10 min exposure to sunlight (B) after 30 min.

exposing to sunlight the silver nitrate solution containing the plant extract for 10 min. Here the 2θ values at 38.4° , 44.6° , 64.8° , 77.6° corresponded to (1 1 1), (2 0 0), (2 2 0) and (3 1 1) reflection of face-centered cubic silver crystal lattice (JCPDS No: 00-004-0783). Since the exposure time is very low, initially formed silver oxide nanoparticles are not fully converted into silver nanoparticles. The 2θ values at 32.5° , 46.5° , 55.1° and 57.8° indexed as (1 1 1), (2 1 1), (2 2 0) and (2 2 1) planes of silver oxide in cubic crystal lattice (JCPDS No: 76-1393). Pure silver nanoparticles were obtained when the solution was exposed to sunlight for 30 min during its preparation. This is evident from its diffraction pattern shown in Fig. 4b(B). Scherrer equation for calculating the average crystallite size of nanoparticle is only applicable if nanoparticle is spherical in nature. From the HRTEM analysis, silver nanoparticles have random shapes like hexagonal, triangular, rod, etc. Hence for silver nanoparticle average crystallite size was not calculated.

3.1.5. Field emission scanning electron microscopy (FESEM) analysis

FESEM image of the CuO nanoparticles is shown in Fig. 5a. It shows that the particles are polydispersed and spherical in nature which was

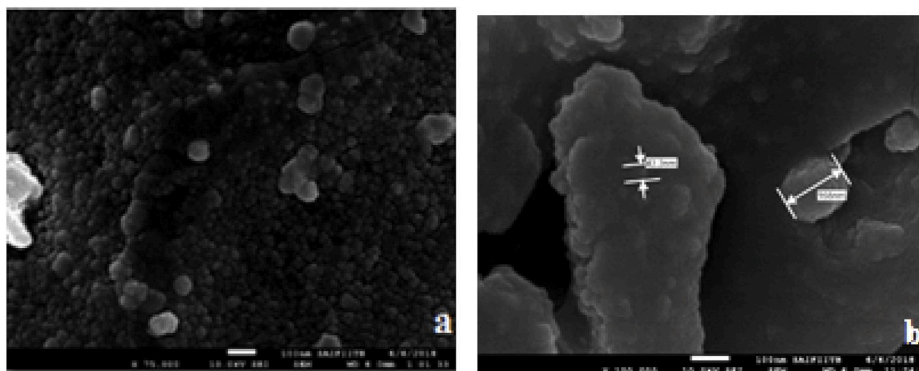


Fig. 5. FESEM image of (a) CuO NPs and (b) Ag NPs.

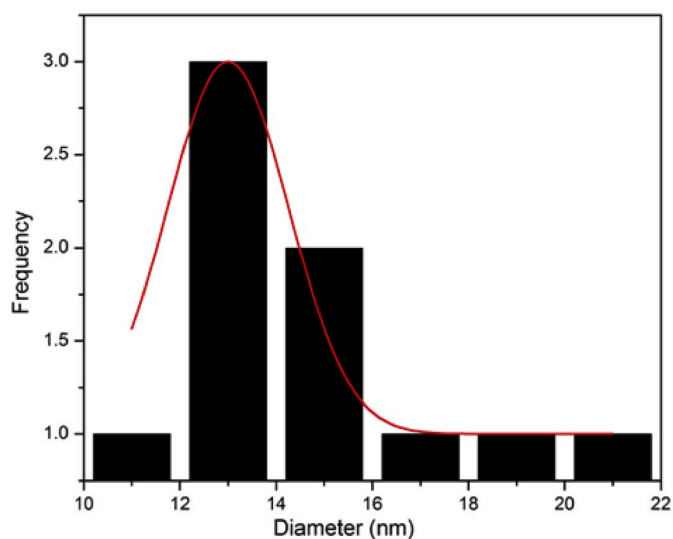


Fig. 6. Particle size distribution histogram of CuO nanoparticles.

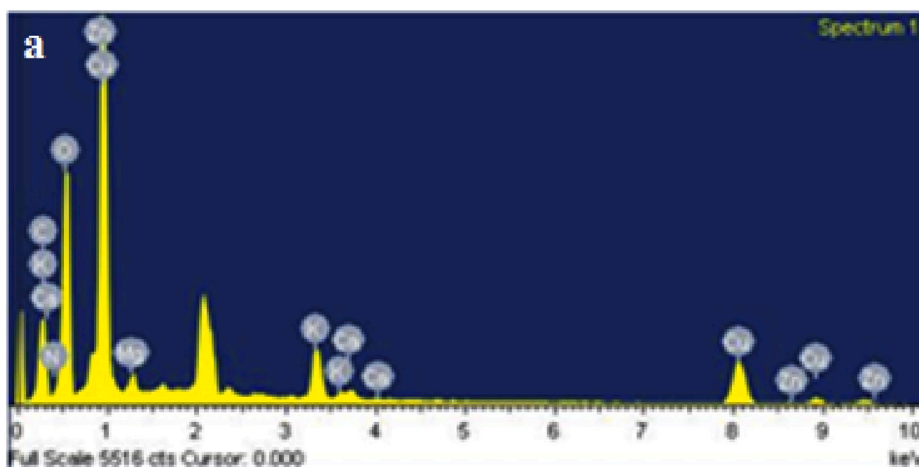


Fig. 7a. EDS spectrum of CuO NPs.

impregnated by the phytoconstituents. Average particle size was found out using histogram as 13 ± 0.63 nm (Fig. 6). The silver nanoparticle was found to be agglomerated clusters under SEM analysis (Fig. 5b). Such aggregation leads to the formation of nanoparticle size more than 100 nm (Baghayeri et al., 2018). Histogram analysis do not hold random shaped nanoparticle.

3.1.6. Energy dispersive X-ray spectroscopy (EDS) analysis

EDS analysis of the biosynthesized nanoparticle helps to find out the elemental composition present in the sample (Fig. 7). In the case of CuO nanoparticle (Fig. 7a), high intense peak at 0.9 and less intense peaks at 8.1 and 8.9 keV represents $\text{CuL}\alpha$, $\text{CuK}\alpha$, and $\text{CuK}\beta$ respectively contributing to a wt% of 44.11%. A strong peak for elemental oxygen was observed at 5 keV with wt% of 33.64% which confirms the

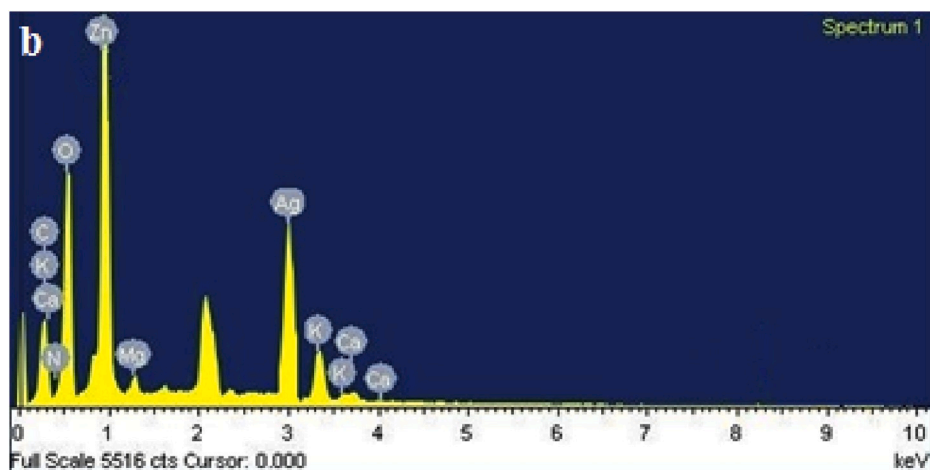


Fig. 7b. EDS spectrum of silver nanoparticle.

formation of CuO. Signals obtained for Na, K, Ca and Zn which is present in the biomolecules that encapsulated the nanoparticles. The peak at 3 keV in the EDS spectrum of silver nanoparticle shows the existence of silver with a wt% of 32.7% (Fig. 7b). The elemental profile of other elements is due to the existence of biomolecules and micronutrients present in the plant extract that had associated with the nanoparticle during its formation.

3.1.7. High-resolution transmission electron microscopy (HRTEM) analysis

Spherical nature of CuO nanoparticle was confirmed by HRTEM analysis (Fig. 8). The copper oxide nanoparticles are evenly distributed with an average particle size of 4 nm. Fig. 8c represents the SAED pattern of the nanoparticle and the sharp rings with bright spot represent the nanocrystalline nature of the sample. The “d” spacing was estimated to be 0.21, 0.13 and 0.10 nm that are respectively the (111), (113) and (022) orientation of monoclinic structure of the metallic CuO nanoparticle.

Shape and size distribution of silver nanoparticle was identified using the HRTEM images and the SAED pattern. It was observed that the silver nanoparticle formed with random shapes that include spherical, hexagonal, triangular, rod etc. The average size of spherically shaped nanoparticle was found to be 31.31 nm. The SAED pattern shows the presence of ring with bright spots originating from (002), (022) and (113) planes of *fcc* lattice indicating nanocrystalline nature of the silver nanoparticles (Fig. 8d).

3.2. Application of CuO and silver nanoparticle

3.2.1. Catalytic activity of CuO NPs in CuAAC reaction

Catalytic activity of the bio-synthesized CuO nanoparticle was investigated for the click synthesis of 1,2,3-triazoles in water. The synthesis of 1,2,3-triazoles was optimized using phenyl acetylene as alkyne, benzyl chloride as halide and sodium azide in presence of the bio-generated copper catalyst. Effect of solvent, time, temperature and catalyst loading were studied (Table 1). Water, ethanol, tetrahydrofuran (THF), *t*-butanol and ethanol/water mixture were tested as solvents. Among these solvents, water shows a significant effect on the yield of triazole. An optimum yield of 96% was obtained within 5 h when 0.01 g of CuO nanoparticle as the catalyst was used in water at 60 °C (Table 1, entry 6). The product formed was separated by filtration followed by recrystallization from ethanol. By increasing the catalyst concentration to 0.02 g, the reaction was completed within 4 h. In order to confirm that

the catalytic activity arises from the copper moiety of the plant generated catalyst, a control experiment for the reaction was also performed by taking the reactants in the absence of any catalyst and the triazole was not formed (Table 1, entry 10).

Encouraged by these results, we further decided to utilise the catalytic activity of the nanoparticles in the click reaction to generate 1,2,3-triazoles using 10 mg of the copper nanocatalyst at 60 °C in water. The results are summarized in (Table 2, entries 1–12).

It appears that the electronic effect of the substituents on the alkyl halide has little effect on the overall yield of the product (Table 2). Lowest yield of the triazole was observed in cyclopentyl bromide (Table 2, entry 6), presumably due to the difficulty in displacing the bromine atom from secondary carbon atom of the cyclopentyl ring. Compared to phenyl acetylene, a slight decrease in the yield of triazole was observed when 4-methyl phenylacetylene was used as the alkyne (Table 2, entries 10–12). Presence of electron releasing methyl group on the phenyl ring increases the electron density at the triple bond making it less effective in attracting the azide towards the cycloaddition reaction.

3.2.2. Reusability of CuO NPs

Using a model reaction of phenylacetylene, benzyl chloride and sodium azide as reactants in water, we have studied the reusability of the CuO nanoparticles as catalyst for the click reaction. It was verified that the CuO nanoparticle was recyclable for the click reaction between phenylacetylene and *in situ* generated phenyl azide. The solid product formed was separated by filtration and recrystallised from ethanol. Since the nanoparticles remain in solution after separation of the product, the filtrate was used as such for the subsequent cycles. The solution was recovered for five times and the triazole was isolated in each step without compromising too much on the yield (Fig. 9).

3.2.3. Effect of silver nanoparticle on microbes

The antimicrobial activity of silver nanoparticle was tested using disc diffusion method against multidrug-resistant human pathogens such as gram-positive bacteria *Bacillus subtilis*, *Staphylococcus aureus* and gram-negative bacteria *Escherichia coli*, *Pseudomonas aeruginosa* (Fig. 10). The zone of inhibition (mm) was then measured after introducing the drugs followed by incubation at 37 °C for 24 h (Table 3).

Silver nanoparticle synthesized by the green method was found to have better antibacterial activity against gram negative bacteria. Among the bacterial stains, *Pseudomonas* (MTCC 2642) showed maximum zone

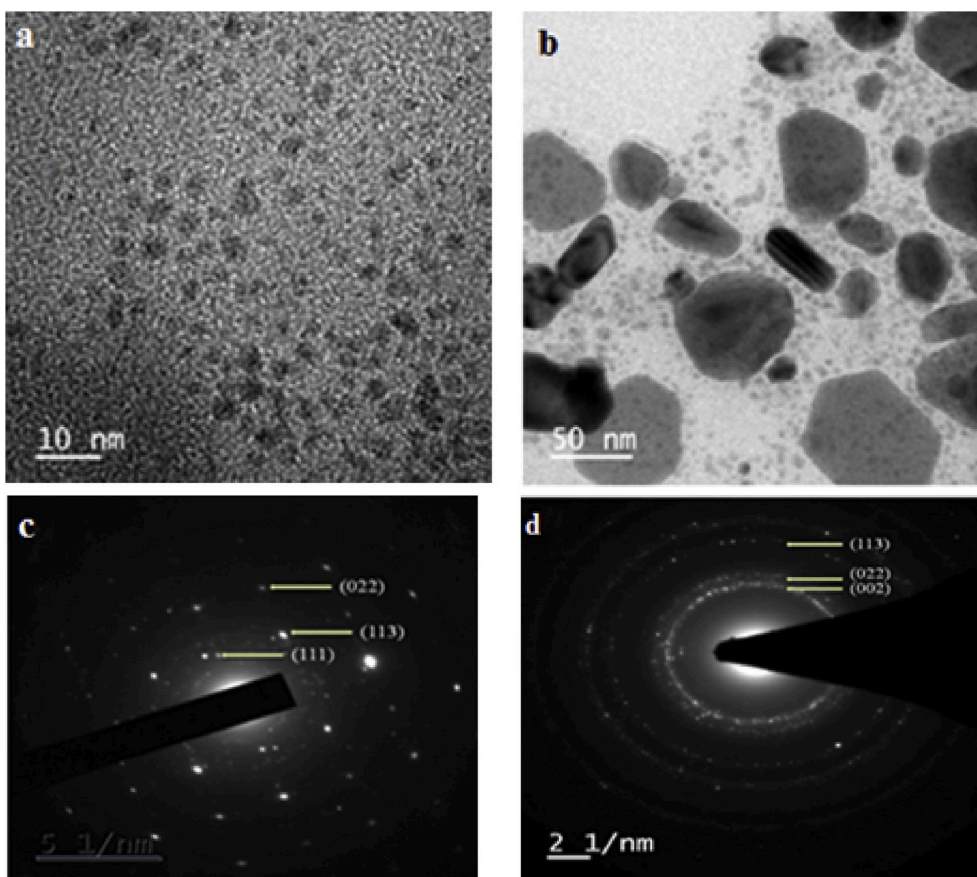
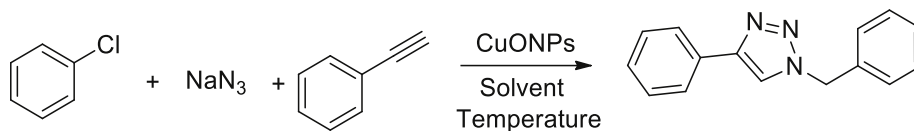


Fig. 8. HR-TEM images of (a) CuO NPs, (b) silver NPs; (c) SAED pattern of CuO and (d) silver NPs.

Table 1
Optimization of the CuAAC reaction^a.

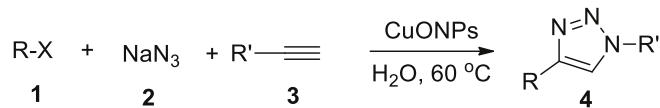


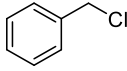
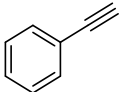
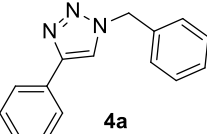
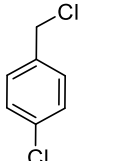
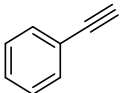
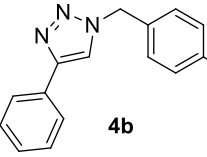
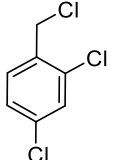
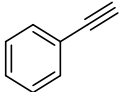
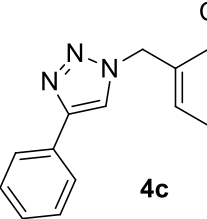
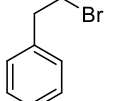
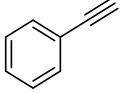
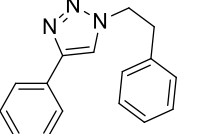
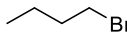
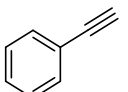
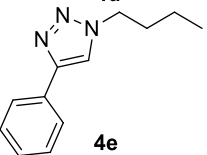
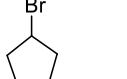
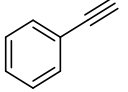
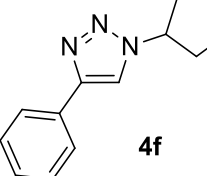
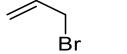
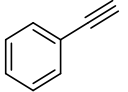
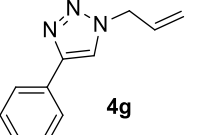
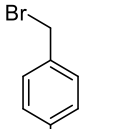
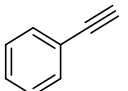
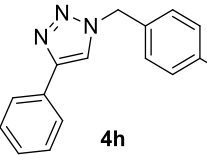
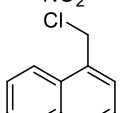
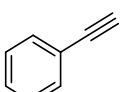
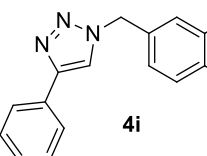
Entry	Catalyst loading(g)	Solvent	Temperature	Time(h)	Yield % ^b
1	0.01	H ₂ O	rt	12	70
2	0.01	Ethanol	rt	48	65
3	0.01	THF	rt	48	40
4	0.01	t-BuOH	rt	20	75
5	0.01	Ethanol/H ₂ O	rt	20	50
6	0.01	H ₂ O	60 °C	5	96
7	0.01	Ethanol	60 °C	5	70
8	0.005	H ₂ O	60 °C	15	90
9	0.02	H ₂ O	60 °C	4	96
10	Nil	H ₂ O	60 °C	10	Nil

^a Reaction conditions: benzyl chloride (1.1 mmol), NaN₃ (1.5 mmol), phenylacetylene (1 mmol) and solvent (5 ml).

^b Isolated yields.

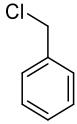
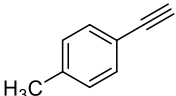
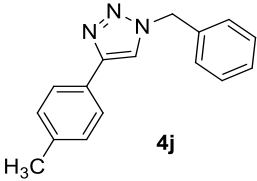
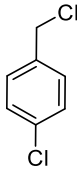
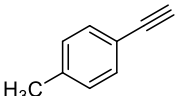
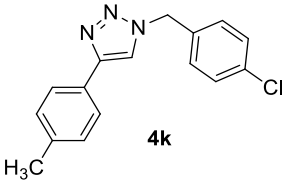
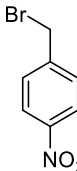
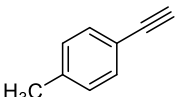
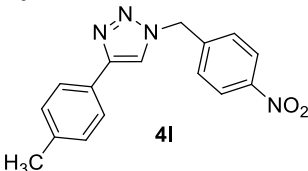
Table 2
 Synthesis of 1,4-disubstituted 1,2,3-triazole using alkyl halide, sodium azide and alkyne^a.



Sl No.	Halide (1)	Alkyne (3)	Product (4)	Yield (%) ^b
1			 4a	96
2			 4b	94
3			 4c	90
4			 4d	96
5			 4e	87
6			 4f	80
7			 4g	88
8			 4h	96
9			 4i	92
10				90

(continued on next page)

Table 2 (continued)

Sl No.	Halide (1)	Alkyne (3)	Product (4)	Yield (%) ^b
11				93
12				94
				

^a Reaction conditions: Halide (1.1 mmol), NaN₃ (1.5 mmol), alkyne (1 mmol) and CuONPs (10 mg) in water (5 ml) at 60 °C for 5 h.

^b Isolated yields.

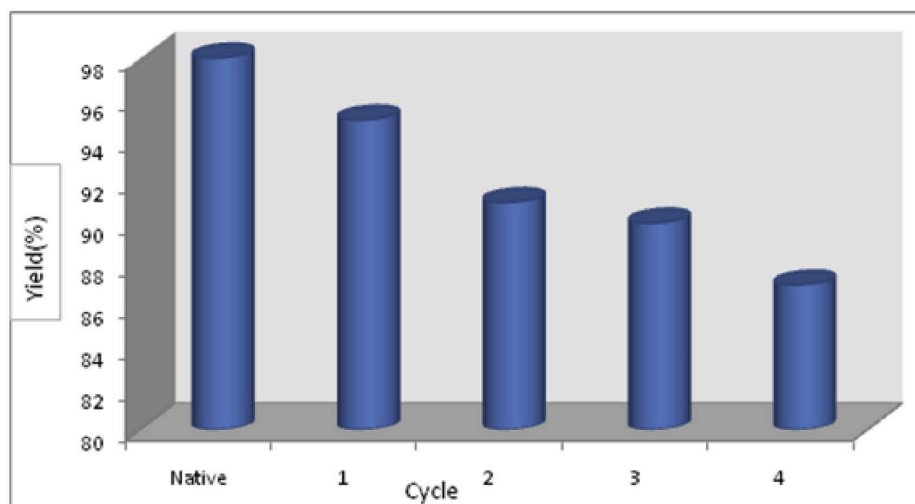


Fig. 9. Reusability of CuO NPs in CuAAC reaction.

of inhibition of 21 mm for 200 μ L whereas its effect was relatively low for *Escherichia coli* (MTCC 68) as 200 μ L produced only 15 mm zone of inhibition. For gram-positive bacteria; *Staphylococcus* (MTCC 3103) and *Bacillus subtilis* (MTCC 869), the silver nanoparticle had almost equal activity in all concentrations. Antibacterial activity of pure silver nanoparticles was compared with silver having small amount of silver oxide and it did not show any noticeable difference in its activity. The generalized mechanism of bacterial stains is due to the interaction of silver ions with phosphorous moieties in DNA (Mijakovic et al., 2006). Crude extract of the pericarp doesn't show any noticeable antibacterial activity against these gram-positive and gram-negative bacteria strains.

4. Conclusion

In conclusion, we have demonstrated a green, cost-effective, rapid synthesis of CuO and silver nanoparticle using *Myristica fragrans* fruit extract. The nanoparticles synthesized were characterized using analytical techniques like FT-IR, UV-Vis, FESEM, EDS, TEM etc. The CuO nanoparticle was found to be an excellent heterogeneous catalyst for CuAAC reaction in water. The catalyst can be recycled and reused five successive cycles with little compromise in the triazole yield. It was observed that the silver nanoparticles synthesized using this method had promising antibacterial activity. These studies can contribute towards an enhanced application of the less economic pericarp of an industrially important *Myristica fragrans* fruit.

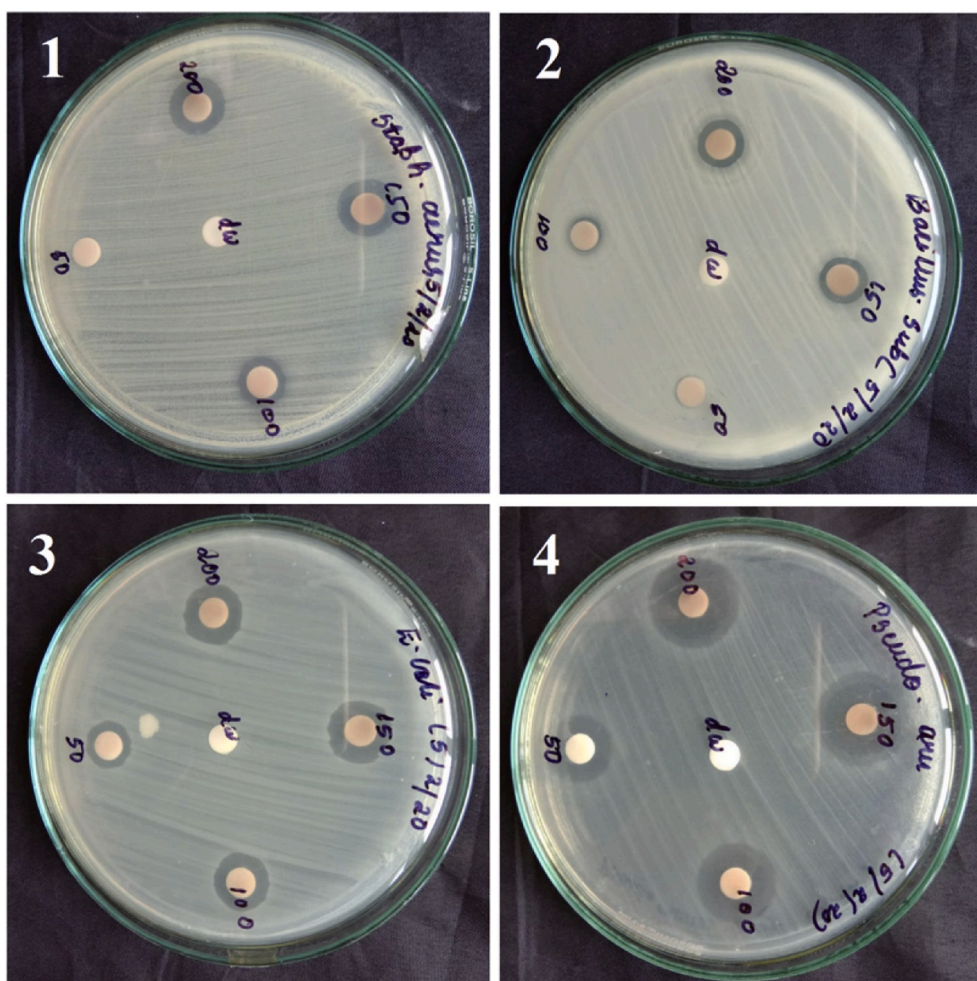


Fig. 10. Antimicrobial activity of AgNPs prepared using *Myristica fragrans* fruit extract against human pathogenic microorganisms (1) *Staphylococcus* sp. (2) *Bacillus* (3) *E.coli* and (4) *Pseudomonas*.

Table 3

Zone of inhibition of silver nanoparticle against bacterial strains.

Drug (µL)	Zone of Inhibition (mm)			
	<i>Staphylococcus</i> (1)	<i>Bacillus</i> (2)	<i>Pseudomonas</i> (3)	<i>E.coli</i> (4)
Dist. Water	0	0	0	0
Streptomycin	16	22	14	11
50	7	8	15	12
100	10	9	18	14
150	12	10	19	15
200	13	11	21	15

Declaration of competing interest

The authors declare that they have no known competing financial interests or personal relationships that could have appeared to influence the work reported in this paper.

CRediT authorship contribution statement

Drishya Sasidharan: Writing - original draft, Data curation. **T.R. Namitha:** Methodology. **Smera P. Johnson:** Investigation, Resources. **Vimala Jose:** Conceptualization, Formal analysis. **Paulson Mathew:** Supervision, Funding acquisition, Writing - review & editing.

Acknowledgements

PM thanks the University Grants Commission (UGC), New Delhi for the generous support for a GCMS system under Innovative Programme (No.F.14-18/2013 Inno/ASIT). We thank SAIF, Cochin University of Science and Technology (CUSAT), Kerala, INDIA for providing NMR and other analytical data.

Appendix A. Supplementary data

Supplementary data to this article can be found online at <https://doi.org/10.1016/j.scp.2020.100255>.

References

- Abdelghany, T.M., Al-Rajhi, A.M., Al Abboud, M.A., Alawlaqi, M.M., Magdah, A.G., Helmy, E.A., Mabrouk, A.S., 2018. Recent advances in green synthesis of silver nanoparticles and their applications: about future directions. A review. *BioNanoScience* 8, 5–16.
- Acuña, U.M., Carcache, P.J.B., Matthew, S., Carcache de Blanco, E.J., 2016. New acyclic bis phenylpropanoid and neolignans, from *Myristica fragrans* Houtt., exhibiting PARP-1 and NF-κB inhibitory effects. *Food Chem.* 202, 269–275.
- Anastas, P.T., Kirchhoff, M.M., 2002. Origins, current status, and future challenges of green chemistry. *Acc. Chem. Res.* 35, 686–694.
- Anseth, K.S., Klok, H.-A., 2016. Click chemistry in biomaterials, nanomedicine, and drug delivery. *Biomacromolecules* 17, 1–3.
- Baghayeri, M., Mahdavi, B., Hosseini-Mohsen Abadi, Z., Farhadi, S., 2018. Green synthesis of silver nanoparticles using water extract of *Salvia lerifolia*: antibacterial

- studies and applications as catalysts in the electrochemical detection of nitrite. *Appl. Organomet. Chem.* 32, e4057.
- Baruwati, B., Varma, R.S., 2009. High value products from waste: grape pomace extract – a three-in-one package for the synthesis of metal nanoparticles. *Chemsuschem* 2, 1041–1044.
- Baruwati, B.B., Polshettiwar, V., Varma, R.S., 2009. Glutathione promoted expeditious green synthesis of silver nanoparticles in water using microwaves. *Green Chem.* 11, 926–930.
- Belushkin, A., Yesilköy, F., Altug, H., 2018. Nanoparticle enhanced plasmonic biosensor for digital biomarker detection in a microarray. *ACS Nano* 12, 4453–4461.
- Bock, V.D., Hiemstra, H., van Maarseveen, J.H., 2006. Cu¹-catalyzed alkyne–azide “click” cycloadditions from a mechanistic and synthetic perspective. *Eur. J. Org. Chem.* 40, 51–68.
- Cho, S.Y., Koh, H.J., Yoo, H.W., Kim, J.S., Jung, H.T., 2017. Tunable volatile-organic-compound sensor by using Au nanoparticle incorporation on MoS₂. *ACS Sens.* 2, 183–189.
- Hebbalalu, D., Lalley, J., Nadagouda, M.N., Varma, R.S., 2013. Greener techniques for the synthesis of silver nanoparticles using plant extracts, enzymes, bacteria, biodegradable polymers, and microwaves. *ACS Sustain. Chem. Eng.* 1, 703–712.
- Huisgen, R., 1963. 1,3-Dipolar cycloadditions. past and future. *Angew. Chem. Int. Ed.* 2, 565–598.
- Jadhav, K., Deore, S., Dhamecha, D., Rajeshwari, H.R., Jagwani, S., Jalalpure, S., Bohara, R., 2018a. Phytosynthesis of silver nanoparticles: characterization, biocompatibility studies, and anticancer activity. *ACS Biomater. Sci. Eng.* 4, 892–899.
- Jadhav, M.S., Kulkarni, S., Raikar, P., Barretto, D.A., Vootla, S.K., Raikar, U.S., 2018b. Green biosynthesis of CuO & Ag–CuO nanoparticles from *Malus domestica* leaf extract and evaluation of antibacterial, antioxidant and DNA cleavage activities. *N. J. Chem.* 42, 204–213.
- Koduru, J.R., Kailasa, S.K., Bhamore, J.R., Kim, K.-H., Dutta, T., Vellingiri, K., 2018. Phytochemical-assisted synthetic approaches for silver nanoparticles antimicrobial applications: a review. *Adv. Colloid Interface Sci.* 256, 326–339.
- Kolb, H.C., Finn, M.G., Sharpless, K.B., 2001. Click chemistry: diverse chemical function from a few good reactions. *Angew. Chem. Int. Ed.* 40, 2004–2021.
- Kou, J., Varma, R.S., 2012. Beet juice utilization: expeditious green synthesis of noble metal nanoparticles (Ag, Au, Pt, and Pd) using microwaves. *RSC Adv.* 2, 10283.
- Lewinski, N., Colvin, V., Drezek, R., 2008. Cytotoxicity of nanoparticles. *Small* 4, 26–49.
- Lutz, J.F., 2007. 1,3-Dipolar cycloadditions of azides and alkynes: a universal ligation tool in polymer and materials science. *Angew. Chem. Int. Ed.* 46, 1018–1025.
- Lutz, J.F., Zarafshani, Z., 2008. Efficient construction of therapeutics, bioconjugates, biomaterials and bioactive surfaces using azide-alkyne “click” chemistry. *Adv. Drug Deliv. Rev.* 60, 958–970.
- Mijakovic, I., Petranovic, D., Mecek, B., Cepo, T., Mann, M., Davies, J., 2006. Bacterial single-stranded DNA-binding proteins are phosphorylated on tyrosine. *Nucleic Acids Res.* 34, 1588–1596.
- Meldal, M.P., Meldal, M., Tornøe, C.W., 2017. Cu-catalyzed azide–alkyne cycloaddition. *Chem. Rev.* 108, 2952–3015.
- Nadagouda, M.N., Varma, R.S., 2006. Green and controlled synthesis of gold and platinum nanomaterials using vitamin B2: density-assisted self-assembly of nanospheres, wires and rods. *Green Chem.* 8, 516–518.
- Nadagouda, M.N., Varma, R.S., 2008. Green synthesis of silver and palladium nanoparticles at room temperature using coffee and tea extract. *Green Chem.* 10, 859–862.
- Nadagouda, M.N., Iyanna, N., Lalley, J., Han, C., Dionysiou, D.D., Varma, R.S., 2014. Synthesis of silver and gold nanoparticles using antioxidants from blackberry, blueberry, pomegranate and turmeric extracts. *ACS Sustain. Chem. Eng.* 2, 1717–1723.
- Nasrollahzadeh, M., Ghorbannezhad, F., Issaabadi, Z., 2019a. Recent developments in the biosynthesis of Cu-based recyclable nanocatalysts using plant extracts and their application in the chemical reactions. *Chem. Rec.* 19, 601–643.
- Nasrollahzadeh, M., Yek, S., Motahharifar, N., Gorab, M.G., 2019b. Recent developments in the plant-mediated green synthesis of Ag-based nanoparticles for environmental and catalytic applications. *Chem. Rec.* 19, 1–45.
- Pandey, R., Mahar, R., Hasanain, M., Shukla, S.K., Sarkar, J., Rameshkumar, K.B., Kumar, B., 2016. Rapid screening and quantitative determination of bioactive compounds from fruit extracts of *Myristica* species and their *in-vitro* antiproliferative activity. *Food Chem.* 211, 483–493.
- Polepalli, S., Rao, C.P., 2018. Drum stick seed powder as smart material for water purification: role of *Moringa oleifera* coagulant protein-coated copper phosphate nanoflowers for the removal of heavy toxic metal ions and oxidative degradation of dyes from water. *ACS Sustain. Chem. Eng.* 6, 15634–15643.
- Saratale, R.G., Karuppusamy, I., Saratale, G.D., Pugazhendhi, A., Kumar, G., Park, Y., Ghodake, G.S., Bharagava, R.N., Banu, J.R., Shin, H.S., 2018. A comprehensive review on green nanomaterials using biological systems: recent perception and their future applications. *Colloids Surf. B Biointerfaces* 170, 20–35.
- Soresh, A., Kwon, F., Taylor, R., Pietrantonio, P., Pine, M., Sayes, C.M., 2011. Surface functionalization of silver nanoparticles: novel applications for insect vector control. *ACS Appl. Mater. Interfaces* 3 (10), 3779–3787.
- Sulaiman, S.F., Ooi, K.L., 2012. Antioxidant and anti food-borne bacterial activities of extracts from leaf and different fruit parts of *Myristica fragrans* Houtt. *Food Contr.* 25, 533–536.
- Sun, X., Li, Y., Li, M.-J., 2019. Highly dispersed palladium nanoparticles on carbon-decorated porous nickel electrode: an effective strategy to boost direct ethanol fuel cell up to 202 mW cm⁻². *ACS Sustain. Chem. Eng.* 7, 11186–11193.
- Thangavel, S., Ramaraj, R., 2008. Polymer membrane stabilized gold nanostructures modified electrode and its application in nitric oxide detection. *J. Phys. Chem. C* 112, 19825–19830.
- Tian, Y., Zhao, Y.Y., Zheng, W.F., Zhang, W., Jiang, X.Y., 2014. Antithrombotic functions of small molecule-capped gold nanoparticles. *Nanoscale* 6, 8543–8550.
- Varma, R.S., 2012. Greener approach to nanomaterials and their sustainable applications. *Curr. Opin. Chem. Eng.* 1, 123–128.
- Xia, Y., Yang, H., Campbell, C.T., 2013. Nanoparticles for catalysis. *Acc. Chem. Res.* 46, 1671–1672.
- Yu, X., Marks, T.J., Facchetti, A., 2016. Metal oxides for optoelectronic applications. *Nat. Mater.* 15, 383–396.
- Zhao, X., Wu, H., Wei, J., Yang, M., 2019. Quantification and characterization of volatile constituents in *Myristica fragrans* Houtt. by gas chromatography-mass spectrometry and gas chromatography quadrupole-time-of-flight mass spectrometry. *Ind. Crop. Prod.* 130, 137–145.
- Zheng, K., Setyawati, M.I., Leong, D.T., Xie, J., 2018. Antimicrobial silver nanomaterials. *Coord. Chem. Rev.* 357, 1–17.